Conformational heterogeneity of the aspartate transporter Glt(Ph)

Hänelt, Inga; Wunnicke, Dorith; Bordignon, Enrica; Steinhoff, Heinz-Juergen; Slotboom, Dirk Jan

Published in:
Nature Structural & Molecular Biology

DOI:
10.1038/nsmb.2471

nature structural & molecular biology

Conformational heterogeneity of the aspartate transporter Glt_{Ph}

Inga Hänelt[1], Dorith Wunnicke[2], Enrica Bordignon[3], Heinz-Jürgen Steinhoff[2] & Dirk Jan Slotboom[1,4]

Glt_{Ph} is a *Pyrococcus horikoshii* homotrimeric Na^+-coupled aspartate transporter that belongs to the glutamate transporter family. Each protomer consists of a trimerization domain involved in subunit interaction and a transporting domain with the substrate-binding site. Here, we have studied the conformational changes underlying transport by Glt_{Ph} using EPR spectroscopy. The trimerization domains form a rigid scaffold, whereas the transporting domains sample multiple conformations, consistent with large-scale movements during the transport cycle. Binding of substrates changed the occupancies of the different conformational states, but the domains remained heterogeneous. The membrane environment favored conformations different from those observed in detergent micelles, but the transporting domain remained structurally heterogeneous in both environments. We conclude that the transporting domains sample multiple conformational states with substantial occupancy regardless of the presence of substrate and coupling ions, consistent with equilibrium constants close to unity between the observed transporter conformations.

Glutamate is the main excitatory neurotransmitter in the brain. It is released into the synaptic cleft and activates ionotropic and metabotropic glutamate receptors in the postsynaptic membrane[1]. Excitatory amino acid transporters (EAATs) in the plasma membranes of cells surrounding the synapse (glial cells and neurons) catalyze the uptake of glutamate and contribute to clearance of the neurotransmitter from the extracellular fluid. Mammalian EAATs belong to a large superfamily of transport proteins found in many eukaryotic and prokaryotic organisms, called the glutamate transporter or ubiquitous solute carrier-1 (SLC1) family[2]. Prokaryotic members are involved in uptake of nutrients that serve as carbon and nitrogen sources. Glutamate transporters are secondary active transporters that couple substrate transport to the transport of cations (sodium ions, potassium ions and protons) across the membrane. Preexisting gradients of these cations allow accumulation of the amino acid substrate in cells. The type and number of co- or counter-transported cations vary among the members of the glutamate transporter family[3–6].

The most extensively studied prokaryotic member of the glutamate transporter family is the aspartate transporter Glt_{Ph}, from *Pyrococcus horikoshii*[7]. This protein couples aspartate transport to the symport of three sodium ions[4]. It also shows substrate-gated chloride conductance[8]. Glt_{Ph} is the only member of the glutamate transporter family for which crystal structures are available[9–12]. Glt_{Ph} is a homotrimeric protein, and its protomers have a complex membrane topology, including two helical hairpins (HP1 and HP2) and broken helices. Each of the three subunits contains a substrate-binding site and a translocation path. Crystal structures of Glt_{Ph} reveal that the protein consists of two domains: a trimerization domain that provides a rigid scaffold[12,13] and a transporting domain. The transporting domain binds the substrates and may undergo a large movement (of ~1.6 nm) during the transport cycle to shuttle the bound and occluded substrates between outward-oriented (1XFH, 2NWL) and inward-oriented (3KBC) states (intermediate state: 3V8G). In addition, smaller movements have been proposed in which HP1 and HP2 could act as lids or gates for substrate binding and release, on the cytoplasmic and extracellular side, respectively[12].

We have used EPR spectroscopy to study the conformational dynamics of Glt_{Ph}. We focused on the question of whether the predicted large-scale movement of the transporting domain indeed takes place, and we studied how the environment (micelles or membranes) and the binding of substrates affect the conformational transitions.

RESULTS

Design of EPR measurements

To monitor the structural changes that occur upon substrate binding by EPR spectroscopy, we used site-directed spin labeling. We created single and double cysteine mutants of Glt_{Ph} that we modified with the reagent 1-oxyl-2,2,5,5-tetramethylpyrroline-3-methyl)methanethiosulfonate (MTSL). **Figure 1** gives an overview of the residues used for site-directed spin labeling. Transport assays using the purified proteins in proteoliposomes showed that all spin-labeled mutants were active in aspartate transport (**Fig. 1e**).

We used a pulsed EPR method (double electron-electron resonance (DEER)) with a working temperature of 50 K to measure distances of 1.5–8 nm between the spin-labeled side chains, and we used continuous wave (CW) EPR experiments with a working temperature

[1]Groningen Biomolecular Science and Biotechnology Institute, University of Groningen, Groningen, The Netherlands. [2]Department of Physics, University of Osnabrück, Osnabrück, Germany. [3]Swiss Federal Institute of Technology Zurich, Laboratory of Physical Chemistry, Zurich, Switzerland. [4]Zernike Institute for Advanced Materials, University of Groningen, Groningen, The Netherlands. Correspondence should be addressed to D.J.S. (d.j.slotboom@rug.nl).

Received 10 July 2012; accepted 20 November 2012; published online 20 January 2013; doi:10.1038/nsmb.2471

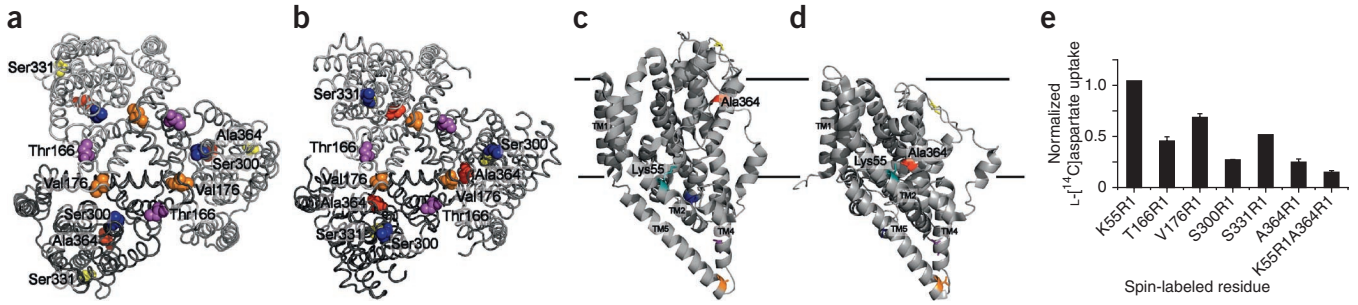

Figure 1 Residues selected for EPR measurements. (**a**–**d**) Ribbon diagrams of Glt_{Ph} trimers as viewed from the cytoplasm (**a**,**b**) and Glt_{Ph} protomers as viewed from the membrane plane (**c**,**d**). TM, transmembrane segment. Black lines (**c**,**d**) indicate the position of the plasma membrane. Transporting domains are shown in the outward-facing orientation (2NWL) (**a**,**c**) and the inward-facing orientation (3KBC) (**b**,**d**). The residues used for cysteine mutagenesis and spin labeling are color-coded: purple, Thr166; orange, Val176; blue, Ser300; yellow, Ser331; red, Ala364; cyan, Lys55. (**e**) L-[^{14}C]aspartate uptake by spin-labeled Glt_{Ph} mutants in proteoliposomes. Rates of uptake of L-[^{14}C]aspartate within 4 min of the start of the reaction were normalized to the activity of the wild-type protein. Error bars represent the lower and higher values of two independent measurements.

of 160 K to qualitatively extract information on interspin distances <1.8 nm (ref. 14). We analyzed Glt_{Ph} both solubilized in detergent micelles and reconstituted in proteoliposomes and compared the results from each experiment type.

The trimerization domain is a stable scaffold

Introduction of a spin label at a single position in Glt_{Ph} allows for the measurement of the distance between the protomers of the homotrimeric protein. We constructed two trimerization-domain mutants by replacing Thr166 (located in the cytoplasmic end of transmembrane helix 4) and Val176 (located in the cytoplasmic end of helix 5) with an MTSL-modified cysteine (R1). Simulations on the available crystal structures indicated that these spin labels are >1.8 nm apart and therefore suitable for DEER measurements[15]. We did not observe spectral broadening in the CW EPR measurements, which further supports the notion that the spin labels were >1.8 nm apart (**Supplementary Fig. 1**). We recorded spectra of the apoprotein and of the protein in the presence of saturating concentrations of Na^+ alone or Na^+ and aspartate. In agreement with previous biochemical and structural data[12,13], the trimerization domain did not show any large-scale conformational changes upon addition of coupling ions or substrate (**Fig. 2**). We observed two sharp peaks (centered around 2.8 nm and 3.8 nm for T166R1 and 2.6 nm and 3.4 nm for V176R1) in the interspin distance distributions for proteins in the presence and absence of substrates. The measured distances were in agreement with the interprotomer distances calculated on the basis of the crystal structures (**Table 1** and **Fig. 2**).

Because Glt_{Ph} is a trimer, each mutation resulted in the presence of three cysteines per protein complex, which could result in a considerable population with three spin labels per trimer, depending on the efficiency of spin labeling (**Supplementary Table 1**). In such cases, the experimental distance distributions obtained by DEER may contain artifacts[16]. We analyzed the effects of three-spin artifacts for the spin-labeled mutants used here (**Supplementary Fig. 2**) and found that they contributed only marginally to the observed experimental distributions.

The transporting domain is conformationally heterogeneous

The mutants S300R1, S331R1 and A364R1 are labeled in the transporting domain at the N-terminal end of transmembrane segment 7, the C-terminal end of transmembrane segment 7 and the C-terminal half of HP2, respectively. The available crystal structures suggest that the intermolecular interspin distances in these mutants differ between the outward- and inward-oriented states. The distance between Ser300 residues from different protomers is shorter in the outward- than in

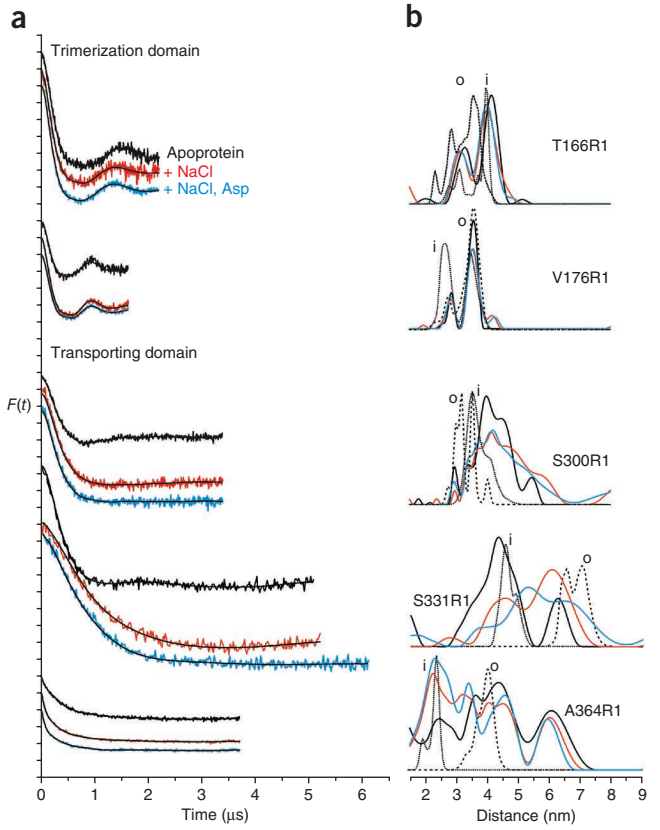

Figure 2 Interprotomer distances in the trimerization and the transporting domains in detergent solution. (**a**,**b**) DEER data of solubilized Glt_{Ph} variants recorded at X band (9.4 GHz; for mutants T166R1, V176R1 and S300R1) or Q band (34 GHz; for mutants S331R1 and A364R1). Data are shown for the apoprotein (black lines) and for the protein in the presence of Na^+ (NaCl; red lines) or Na^+ and aspartate (NaCl, Asp; blue lines). Normalized background-corrected dipolar evolution data $F(t)$ are shown in **a**; tick marks are separated by 0.1. Distance distributions obtained by Tikhonov regularization and by a rotamer library analysis[15] of the inward-facing (i, dotted lines) and outward-facing (o, dashed lines) crystal structures are shown in **b**.

Table 1 Theoretical and experimental distances in the EPR measurements

Residue	Experimental mean interspin distance (nm)			Cα-Cα (nm)	Rotamer library approach (nm)
	–	+ NaCl	+ NaCl and aspartate		
T166R1	3.86 (s)	3.81 (s)	3.76 (s)	2.74 (o)	2.85, 3.55 (o)
				2.99 (i)	3.1, 3.95 (i)
V176R1	3.41 (s)	3.46 (s)	3.47 (s)	2.25 (o)	2.7, 3.55 (o)
	3.40 (r)	3.46 (r)	3.47 (r)	2.21 (i)	2.65, 3.5 (i)
S300R1	4.21 (s)	4.54 (s)	4.42 (s)	3.32 (o)	3.2, 3.55 (o)
				4.43 (i)	3.55, 4.1 (i)
S331R1	4.68 (s)	5.8 (s)	5.97 (s)	7.34 (o)	6.55, 7.05 (o)
	5.3 (r)	5.7 (r)	5.7 (r)	4.7 (i)	4.55, 4.9 (i)
A364R1	3.79 (s)	3.08 (s)	2.93 (s)	4.8 (o)	3.95 (o)
	4.2 (r)	3.6 (r)	3.5 (r)	3.4 (i)	1.95, 2.4 (i)
K55R1 A364R1	>2 (75%),	>2 (45%),	>2 (38%),	2.74 (o)	1.95, 2.6 (o)
solubilized	1.3 (25%)	1.4 (55%)	1.3 (62%)	0.73 (i)	1.2 (i)
K55R1 A364R1	<1.2*	<1.2*	>2 (20%),	2.74 (o)	1.95, 2.6 (o)
reconstituted			1.3 (80%)	0.73 (i)	1.2 (i)

Experimentally determined mean interspin distances, derived from DEER analysis (for single mutants) or from DIPFIT (for K55R1 A364R1), for the detergent-solubilized (s) and liposome-reconstituted (r) apoprotein (–) or protein in the presence of Na^+ alone or Na^+ and aspartate. Cases in which CW spectra were recorded and no dipolar broadening was observed were assigned a distance of >2 nm. For K55R1 A364R1, the percentage of the fractions with and without dipolar broadening is given in brackets. Distance values estimated from the spectral second moment[20] (denoted with asterisk) indicate the presence of interspin distances <1.2 nm. Distance distribution width was fixed to 0.3 nm for the fittings of the CW EPR spectra. Cα-Cα, distances as shown by the crystal structures[10,12]; rotamer library approach, the corresponding major distances resulting from the rotamer library approach as implemented in MMM (o, outward-oriented conformation; i, inward-oriented conformation).

the inward-oriented state (Cα-Cα = 3.3 nm and 4.4 nm, respectively), whereas the opposite is true for Ala364 and Ser331 (for Ala364, Cα-Cα = 4.8 nm and 3.4 nm, respectively; for Ser331, Cα-Cα = 7.3 nm and 4.7 nm, respectively). The experimentally determined distance distributions for all three mutants were very broad or characterized by multiple peaks (**Fig. 2**), indicating conformational heterogeneity in the transporting domain in the apo state. The distance distributions were sensitive to the binding of Na^+ alone or Na^+ and aspartate, but in all cases, the conformational heterogeneity remained (**Fig. 2**). The observed broad features in the interspin distance distributions indicate the presence of multiple conformations, but deconvolution of the resulting distance distribution is difficult owing to overlapping effects arising from intrinsic orientational distribution of the rotamers of the spin label, conformational heterogeneity of the protein and, possibly, effects from background-correction artifacts in DEER. To qualitatively assess the effects of substrate binding, we compared the experimental interprotomer distances with those predicted by the crystal structures for the inward- and outward-facing orientations (**Fig. 2**). In addition, we calculated the means of the experimental distance distributions to provide an indication of the average direction of the distance changes upon addition of substrates (**Table 1**). For S300R1, we observed a slight shift in the broad experimental distance distribution (centered at 4.2 nm in the apo state) toward longer distances upon binding of the Na^+ coupling ion alone as well as Na^+ and aspartate, which suggests a higher occupancy of the inward-facing conformation in the substrate-bound form. In contrast, for S331R1, the binding of Na^+ alone or Na^+ together with aspartate shifted the broad bimodal distribution toward a higher occupancy of the longer distances characteristic of the outward-facing structure. A364R1 also showed a bimodal distribution in the apo state, and this distribution shifted toward the short distances predicted in the inward-facing state in the presence of Na^+ alone and Na^+ and aspartate. Both in the presence and in the absence of substrate, the experimentally determined distances were broader than those calculated from the crystal structures, which could indicate that the trimerization and transporting domains are more loosely associated in solution than in the crystals or that additional conformations not represented by the available crystal structures are present.

Intra-protomer distance measurements

The double cysteine mutant K55C A364C has been used to solve the crystal structure of inward-oriented Glt_{Ph} through cross-linking of the two residues using Hg^{2+} (ref. 12). To further study the relative occupancy of the different conformational states of Glt_{Ph}, we spin labeled K55C A364C and used CW EPR lineshape analysis to obtain distance information. This technique is less sensitive than DEER for determining multiple distance distributions, but in the K55R1 A364R1 variant, the distance between the spin labels is expected to be <1.8 nm only in the inward-oriented conformation (**Supplementary Fig. 3c**); therefore, it was possible to selectively measure the occupancy of this conformational state by CW EPR. In contrast, DEER analysis of the doubly spin-labeled mutant is complicated by the overlap of intra- and interprotomer distances (**Supplementary Fig. 3**).

The spectra of the doubly spin-labeled mutant were dipolar broadened compared to the sum of singly labeled mutants, in the absence of substrate and in the presence of Na^+ or Na^+ together with aspartate (**Fig. 3**), indicating that a fraction of spin labels were <2 nm apart in all cases. The spectra showed an increased broadening in the presence of Na^+ as compared to the apo state, which was even more pronounced in the presence of both Na^+ and aspartate. The increase in dipolar broadening indicates a decrease in the distance, which indicates that a higher fraction of the protein is in the inward-facing conformation.

The membrane environment affects the protein conformations

All measurements described above were performed using detergent-solubilized proteins. To explore the effects of the environment on the conformational transitions of Glt_{Ph}, we reconstituted spin-labeled mutants in liposomes. We selected Glt_{Ph} variants carrying mutations V176R1 (located in the trimerization domain of Glt_{Ph}), S331R1 or A364R1 (located in the transporting domain) and the K55R1 A364R1 double mutant to study distance distributions in proteoliposomes (**Figs. 3** and **4**). V176R1 showed the same distance distribution in the membrane as in detergent solution (**Table 1** and **Supplementary Fig. 4**), regardless of substrate binding. In contrast, for mutants S331R1 and A364R1, the interspin distances were different in proteoliposomes compared to detergent solution. Both mutants showed heterogeneous

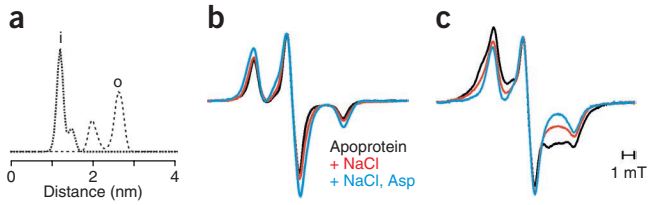

Figure 3 Intra-protomer distances between the trimerization domain and the transporting domain. (**a**) Simulated intra-protomer distances between the spin labels in K55R1 A364R1 in the inward-facing (i) and outward-facing (o) conformations. (**b**,**c**) Low-temperature continuous-wave EPR spectra measured at X band (9.4 GHz) for the detergent-solubilized (**b**) or membrane-reconstituted (**c**) apoprotein (black lines) or protein in the presence of Na^+ (NaCl; red line) or Na^+ and aspartate (NaCl, Asp; blue line).

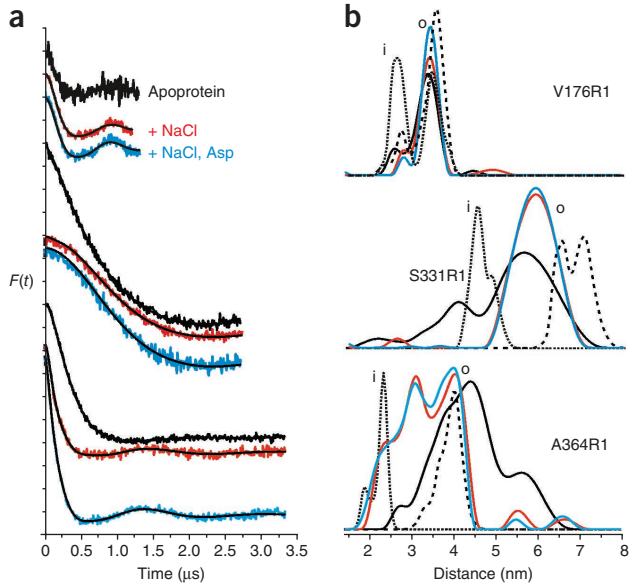

Figure 4 Interprotomer distances in the trimerization and transporting domains in proteoliposomes. (**a**,**b**) DEER data of Glt_{Ph} variants in proteoliposomes recorded at X band (9.4 GHz, for mutant V176R1) or Q band (34 GHz, for mutants S331R1 and A364R1) for the apoprotein (black lines) or in the presence of Na^+ alone (NaCl; red lines) or Na^+ and aspartate (NaCl, Asp; blue lines). Normalized background-corrected dipolar evolution data $F(t)$ are shown in **a**; tick marks are separated by 0.1. Distance distributions obtained by Tikhonov regularization and by a rotamer library analysis[15] of the inward-facing (i, dotted lines) and outward-facing (o, dashed lines) crystal structures are shown in **b**.

distance distributions in detergent and in the membrane, but the extreme distances were suppressed in the membrane, and intermediate distances appeared. For mutant A364R1, the mean distances between the spin labels decreased with addition of coupling ions or substrate (4.2 nm in the apo state, 3.6 nm in presence of Na^+ and 3.5 nm with Na^+ and aspartate present) (**Fig. 4** and **Table 1**). The changes were qualitatively similar to those observed in micelles; however, the change in mean distance (Δd) was only –0.7 nm in proteoliposomes compared to –0.9 nm in the solubilized protein (**Table 1**). This observation indicates that the main conformational changes were smaller in liposomes and that some of the extreme conformations observed in the crystal structure are sampled less frequently in the membrane environment. We observed a similar effect for mutant S331R1, in which the mean distance increased from 5.3 nm to 5.7 nm with substrate and coupling ion addition, resulting in a Δd of 0.4 nm, smaller than that found in micelles (Δd = 1.3 nm) (**Table 1**). The notion that the extreme conformations are sampled less frequently in the membrane environment is also supported by the intra-protomer measurements of spin distances in mutant K55R1 A364R1. Notably, the presence of strong spin-spin (dipolar and Heisenberg) interactions in the apoprotein indicates distances in the 1-nm range (**Fig. 3**). Binding of Na^+ alone or Na^+ and aspartate reduced the spectral broadening, indicating an increase in average interspin distances. Thus, in mutant K55R1 A364R1 in proteoliposomes, substrate addition induced opposite distance changes compared to K55R1 A364R1 in micelles, highlighting the role of the environment in the stabilization of particular conformations.

DISCUSSION

The EPR measurements show that the trimerization domains form the stable core of trimeric Glt_{Ph}, both in detergent solution and in a membrane environment. The rigidity of the trimerization domain is consistent with crystallographic and functional data[12,13]. In contrast, the transporting domains are not captured in a single conformation; rather, they sample multiple conformations, in both the presence and absence of substrate (aspartate) and coupling ions (Na^+). In detergent solution, Glt_{Ph} samples the inward-facing (3KBC) and outward-facing (2NWL) conformations, consistent with the conformations caught in the crystal structures. In contrast, different, intermediate conformations were preferred in the membrane, and these could be similar to those found in an asymmetric crystal structure[9] in which the protomers of the trimer were in different conformations. Occupancy of the conformational states was affected by binding of coupling ions and substrate, as well as by the detergent or lipid environment, but multiple conformational states were sampled in all conditions tested. These observations suggest that the equilibrium constants between the observed transporter conformations are close to unity and, consequently, that different states are populated to similar extents. This observation makes sense for the empty carrier and for Glt_{Ph} bound to both Na^+ and aspartate[17], as these forms need to be able to isomerize between outward- and inward-facing states for substrate binding and release. However, the Na^+-bound protein would not be expected to alternately expose the binding site, as this would lead to uncoupled Na^+ leaks. Nonetheless, multiple conformational states were sampled in the Na^+-loaded carrier as well. Our interpretation of the EPR results is that the transporting domain is constantly shuttling across the membrane, a prerequisite for alternately exposing the binding site. We suggest that local rearrangements like those shown for HP2 (refs. 12,18) trigger the alternating accessibility of the binding sites by coordinately opening and closing the inward- and outward-facing lids or gates, and that the gating is dependent on the presence of substrate and coupling ions. Cross-linking studies on human EAAT1 support the observation that large conformational changes take place in both the presence and the absence of substrates[19].

Notably, the binding of coupling ions and substrate resulted in apparently opposite effects in different spin-labeled mutants in the transporting domain. In mutants S300R1 and A364R1, binding of both Na^+ alone and Na^+ and aspartate caused an increase in occupancy of the inward-oriented state as compared to the apoprotein, whereas mutant S331R1 showed a change in the opposite direction. The occupancy of the states is apparently sensitive to insertion of a cysteine, modification by spin labeling or, possibly, to the freezing that is required to extract distance information by EPR. Again, these observations are consistent with an equilibrium constant close to unity between the observed transporter conformations, a condition in which small perturbations may affect the population of the states.

The available crystal structures of Glt_{Ph} have yielded unprecedented insight into the transport mechanism by providing snapshots of extreme and intermediate conformations. We have compared the conformations of Glt_{Ph} in detergent solution and membranes and have concluded that the large conformational changes suggested by the crystal structures can also be observed in these environments, but that the membrane and the micelle favor different conformations. Moreover, we find that subtle modifications in the protein can have pronounced effects on the equilibrium of the outward- and inward-facing conformations.

METHODS

Methods and any associated references are available in the online version of the paper.

Note: Supplementary information is available in the online version of the paper.

ACKNOWLEDGMENTS
We thank R.H. Duurkens for performing uptake experiments, C. Rickert, D. Klose and J. Klare for help with the EPR measurements and B. Poolman for constructive criticism. This work was supported by a research fellowship and by a research grant from the Deutsche Forschungsgemeinschaft (HA 6322/1-1 to I.H. and STE 640/10, SFB944 to D.W. and H.-J.S.), the Netherlands Organisation for Scientific Research (NWO Vidi and Vici grant to D.J.S.) and the European Union (EDICT program and European Research Council starting grant to D.J.S.).

AUTHOR CONTRIBUTIONS
I.H. and D.J.S. designed the experiments. I.H., D.W. and E.B. conducted the experiments. All authors contributed to writing the manuscript and analyzing the data.

COMPETING FINANCIAL INTERESTS
The authors declare no competing financial interests.

Published online at http://www.nature.com/doifinder/10.1038/nsmb.2471.
Reprints and permissions information is available online at http://www.nature.com/reprints/index.html.

1. Tzingounis, A.V. & Wadiche, J.I. Glutamate transporters: confining runaway excitation by shaping synaptic transmission. *Nat. Rev. Neurosci.* **8**, 935–947 (2007).
2. Slotboom, D.J., Konings, W.N. & Lolkema, J.S. Structural features of the glutamate transporter family. *Microbiol. Mol. Biol. Rev.* **63**, 293–307 (1999).
3. Teichman, S., Qu, S. & Kanner, B.I. The equivalent of a thallium binding residue from an archeal homolog controls cation interactions in brain glutamate transporters. *Proc. Natl. Acad. Sci. USA* **106**, 14297–14302 (2009).
4. Groeneveld, M. & Slotboom, D.J. Na^+:aspartate coupling stoichiometry in the glutamate transporter homologue Glt(Ph). *Biochemistry* **49**, 3511–3513 (2010).
5. Zerangue, N. & Kavanaugh, M.P. Flux coupling in a neuronal glutamate transporter. *Nature* **383**, 634–637 (1996).
6. Raunser, S. *et al.* Structure and function of prokaryotic glutamate transporters from *Escherichia coli* and *Pyrococcus horikoshii*. *Biochemistry* **45**, 12796–12805 (2006).
7. Ryan, R.M., Compton, E.L. & Mindell, J.A. Functional characterization of a Na^+-dependent aspartate transporter from *Pyrococcus horikoshii*. *J. Biol. Chem.* **284**, 17540–17548 (2009).
8. Ryan, R.M. & Mindell, J.A. The uncoupled chloride conductance of a bacterial glutamate transporter homolog. *Nat. Struct. Mol. Biol.* **14**, 365–371 (2007).
9. Verdon, G. & Boudker, O. Crystal structure of an asymmetric trimer of a bacterial glutamate transporter homolog. *Nat. Struct. Mol. Biol.* **19**, 355–357 (2012).
10. Boudker, O., Ryan, R.M., Yernool, D., Shimamoto, K. & Gouaux, E. Coupling substrate and ion binding to extracellular gate of a sodium-dependent aspartate transporter. *Nature* **445**, 387–393 (2007).
11. Yernool, D., Boudker, O., Jin, Y. & Gouaux, E. Structure of a glutamate transporter homologue from *Pyrococcus horikoshii*. *Nature* **431**, 811–818 (2004).
12. Reyes, N., Ginter, C. & Boudker, O. Transport mechanism of a bacterial homologue of glutamate transporters. *Nature* **462**, 880–885 (2009).
13. Groeneveld, M. & Slotboom, D.J. Rigidity of the subunit interfaces of the trimeric glutamate transporter GltT during translocation. *J. Mol. Biol.* **372**, 565–570 (2007).
14. Steinhoff, H.J. Inter- and intra-molecular distances determined by EPR spectroscopy and site-directed spin labeling reveal protein-protein and protein-oligonucleotide interaction. *Biol. Chem.* **385**, 913–920 (2004).
15. Polyhach, Y., Bordignon, E. & Jeschke, G. Rotamer libraries of spin labelled cysteines for protein studies. *Phys. Chem. Chem. Phys.* **13**, 2356–2366 (2011).
16. Jeschke, G., Sajid, M., Schulte, M. & Godt, A. Three-spin correlations in double electron-electron resonance. *Phys. Chem. Chem. Phys.* **11**, 6580–6591 (2009).
17. Boudker, O. & Verdon, G. Structural perspectives on secondary active transporters. *Trends Pharmacol. Sci.* **31**, 418–426 (2010).
18. Focke, P.J., Moenne-Loccoz, P. & Larsson, H.P. Opposite movement of the external gate of a glutamate transporter homolog upon binding cotransported sodium compared with substrate. *J. Neurosci.* **31**, 6255–6262 (2011).
19. Jiang, J., Shrivastava, I.H., Watts, S.D., Bahar, I. & Amara, S.G. Large collective motions regulate the functional properties of glutamate transporter trimers. *Proc. Natl. Acad. Sci. USA* **108**, 15141–15146 (2011).
20. Radzwill, N., Gerwert, K. & Steinhoff, H.J. Time-resolved detection of transient movement of helices F and G in doubly spin-labeled bacteriorhodopsin. *Biophys. J.* **80**, 2856–2866 (2001).

ONLINE METHODS

Mutagenesis, expression, purification and labeling of Glt_{Ph}. Cysteine mutants were introduced in recombinant Glt_{Ph} possessing a C-terminal eight-histidine tag using site-directed mutagenesis. DNA sequencing confirmed the presence of only the desired mutations. Glt_{Ph} was overproduced in *Escherichia coli* MC1061 and purified as previously described[4], with slight modifications. Buffer A containing 50 mM Tris-HCl (pH 8.0), 300 mM KCl and 0.04% (wt/vol) n-dodecyl-β-D-maltopyranoside (DDM) (Anatrace) was used throughout the purification process after solubilization, including size-exclusion chromatography on a Superdex200 column (GE Healthcare). For site-directed spin labeling, the protein was bound to the Ni^{2+}-Sepharose column in the presence of 5 mM 2-mercaptoethanol and subsequently washed with degassed buffers only. Protein bound to Ni^{2+}-Sepharose was labeled overnight at 4 °C with 1 mM (1-oxyl-2,2,5,5-tetramethylpyrrolidin-3-yl)methylmethanethiosulfonate spin label (MTSL) (Toronto Research Chemicals, Inc.). Subsequently, size-exclusion chromatography was performed to remove free spin label. Before labeling, protein concentrations were determined using the calculated extinction coefficients.

Protein reconstitution and transport of [^{14}C]aspartate into proteoliposomes. Reconstitution of Glt_{Ph} mutants into proteoliposomes and transport of [^{14}C]aspartate were performed as previously described[4], with the following modifications: spin-labeled cysteine mutants were reconstituted into a mixture of synthetic lipids (Avanti Polar Lipids, Inc.) of a 3:1:1 weight ratio of 1,2-dioleoyl-*sn*-glycero-3-phosphoethanolamine (DOPE); 1,2-dioleoyl-*sn*-glycero-3-phosphocholine (DOPC); and 1,2-dioleoyl-*sn*-glycero-3-phospho-(1′-*rac*-glycerol) (DOPG). The transport of aspartate was initialized by diluting 2 µl of proteoliposomes (125 µg/µl lipid concentration) loaded with 50 mM KP_i buffer (pH 7) into 200 µl 50 mM sodium phosphate buffer (pH 7) containing 0.69 µM [^{14}C]aspartate and 0.5 µM valinomycin.

EPR measurements. Spin-labeled mutants were concentrated via Vivaspin columns (cutoff 100 kDa, Sartorius) to 100–200 µM and washed two times with buffer A in D_2O, supplemented when indicated with 1 M NaCl or 1 M NaCl and 100 µM aspartate. For spin-labeled mutants reconstituted into liposomes, the proteoliposomes were suspended to a concentration of ~100 µM in 50 mM potassium phosphate buffer containing 0.5 µM valinomycin in D_2O (pH 7). 1 M NaCl, or 1 M NaCl and 100 µM aspartate, were present when indicated. Liposomes were frozen in liquid nitrogen immediately after resuspension. X-band CW EPR spectra at room temperature were recorded using a homemade EPR spectrometer equipped with a dielectric resonator (Bruker) (1 mW microwave power; 0.15 mT B-field modulation amplitude). Sample volumes of 10 µl were placed in EPR glass capillaries. X-band CW EPR spectra at 160 K were carried out using a homemade EPR spectrometer equipped with a Super High Sensitivity Probehead (Bruker) (0.2 mW microwave power; 0.25 mT B-field modulation amplitude), a continuous flow helium cryostat (Oxford Instruments) and a temperature controller (Oxford Instruments). An RMN 2 B-field meter (Drusch) allowed measurement of the magnetic field. Sample volumes of 30–40 µl were loaded into EPR quartz capillaries and frozen in liquid nitrogen before insertion into the resonator.

Pulsed EPR experiments were performed at X band at 50 K on an Elexsys 580 spectrometer (Bruker) equipped with a continuous-flow helium cryostat (Oxford Instruments) in combination with a temperature controller (Oxford Instruments). The four-pulse DEER sequence was applied[21]. All parameters were kept unmodified with respect to previously described values[22], with observer pulses of 16–32 ns and a pump pulse of 12 ns. Sample volumes of 30–40 µl were loaded into EPR quartz tubes (3 mm outer diameter) and shock frozen in liquid nitrogen. The same 3-mm tubes were used to measure Q-band DEER at 50 K in a homemade spectrometer equipped with a 150 W TWT (traveling-wave tube) and an oversized resonator. All pulses were set to 12 ns, and the frequency separation was set to 100 MHz (ref. 23).

Fitting of experimental CW EPR data. Simulated dipolar broadened EPR spectra were fitted to experimental low temperature CW EPR spectra considering a Gaussian distribution of interspin distances using DipFit[24]. Best-fit parameters for interspin distance distributions were determined. The g tensor values, the A_{xx} and A_{yy} values of the hyperfine tensor and the Lorentzian and Gaussian linewidth parameters were fixed to values found for the reference spectra of mutant A364R1 in detergent-solubilized and liposome-reconstituted forms, respectively. EPR spectra were convoluted with a field-independent lineshape function composed of a superposition of 50% Lorentzian and 50% Gaussian shapes of widths 0.37 mT and 0.32 mT, respectively.

DEER analysis. The DEER traces were background corrected using a homogeneous three-dimensional spin distribution. Interspin distance distributions were derived by fitting the background-corrected dipolar evolution function using Tikhonov regularization as implemented in DEERAnalysis2011 (ref. 25). Validation of distance distributions were carried out with the included validation tool. For the mutant A364R1 in detergent micelles, which showed an invariant peak at about 6 nm in all conditions, changes to the background dimensionality during validation resulted in a pronounced variability of the peak intensity. We thus consider the 6-nm peak to be affected by background artifacts, and we did not consider it in the calculation of the mean distances in **Table 1**. The lower spin concentration of the reconstituted samples allowed for the extraction of a reliable background function in all cases, and the validation confirmed the distance distribution presented.

Rotamer library approach. Distance distributions were simulated using a rotamer library approach (RLA) as implemented in MMM[15]. The rotamer library consists of 210 precalculated rotamers representing an ensemble of possible spin-label side chain (R1) conformations at 175 K. The orientation of R1 introduced at the chosen residue with regard to the protein structure permits calculation of the energy for the R1-protein interaction in consideration of the Lennard-Jones potential[26]. Multiplication of the probability for each rotamer (determined by Boltzmann weighting and normalization by the partition function) with the probability that R1 will exhibit this conformation leads to the rotamer probability distribution for a specific residue. Interspin distance distributions are calculated as the histogram of all pairwise interspin distances weighted by the product of their respective probabilities. The three-spin effects on the DEER $F(t)$ traces were also calculated with MMM, and the simulated $F(t)$ traces were subsequently analyzed with DeerAnalysis2011 to obtain the artifacts on the distance distribution for 100% labeling efficiency.

21. Pannier, M., Veit, S., Godt, A., Jeschke, G. & Spiess, H.W. Dead-time free measurement of dipole-dipole interactions between electron spins. *J. Magn. Reson.* **142**, 331–340 (2000).
22. Hänelt, I. *et al.* Membrane region M2C2 in subunit KtrB of the K^+ uptake system KtrAB from *Vibrio alginolyticus* forms a flexible gate controlling K^+ flux: an electron paramagnetic resonance study. *J. Biol. Chem.* **285**, 28210–28219 (2010).
23. Polyhach, Y. *et al.* High sensitivity and versatility of the DEER experiment on nitroxide radical pairs at Q-band frequencies. *Phys. Chem. Chem. Phys.* **14**, 10762–10773 (2012).
24. Steinhoff, H.J. *et al.* Determination of interspin distances between spin labels attached to insulin: comparison of electron paramagnetic resonance data with the X-ray structure. *Biophys. J.* **73**, 3287–3298 (1997).
25. Jeschke, G. *et al.* DeerAnalysis2006—a comprehensive software package for analyzing pulsed ELDOR data. *Appl. Magn. Reson.* **30**, 473–498 (2006).
26. Mackerell, A.D. Jr., Feig, M. & Brooks, C.L. III. Extending the treatment of backbone energetics in protein force fields: limitations of gas-phase quantum mechanics in reproducing protein conformational distributions in molecular dynamics simulations. *J. Comput. Chem.* **25**, 1400–1415 (2004).